



## Article

# Investigation of Acoustic Signals for Gait Analysis

Jeffrey Buxton <sup>1</sup>, Kelly J. Shields <sup>2</sup> , Jesse T. Greyshock <sup>3</sup>, Jared Ramsey <sup>4</sup>, Christopher Adams <sup>5</sup>  
and Geo. A. Richards <sup>6,\*</sup>

<sup>1</sup> Exercise Science Department, Grove City College, Grove City, PA 16127, USA; buxtonjd@gcc.edu

<sup>2</sup> Data Science R&D, Highmark Health, Pittsburgh, PA 15222, USA; kelly.shields@highmarkhealth.org

<sup>3</sup> Bell Textron Inc., Fort Worth, TX 76118, USA; jessegreyshock@gmail.com

<sup>4</sup> Allegheny Orthopedic Associates, Pittsburgh, PA 15241, USA; jared.ramsey@ahn.org

<sup>5</sup> Department of Pediatrics, Pediatric Resident, Akron Children's Hospital, Akron, OH 44308, USA; cadams4@akronchildrens.org

<sup>6</sup> Mechanical Engineering Department, Grove City College, Grove City, PA 16127, USA

\* Correspondence: richardsga@gcc.edu

**Abstract: Background:** Previous literature has demonstrated that footstep sounds can be related to the unique gait pattern of individuals. This paper investigates the potential of using footstep sounds as a diagnostic tool in gait analysis. **Methods:** Fifteen participants ran on a treadmill at 2.7 m/s (6.0 MPH) while simultaneously recording plantar pressure and acoustic signals. Participants repeated the same recordings after completing an exhaustive fatigue protocol, thereby creating a modified gait pattern. **Results:** The modified gait was evident in the center-of-force trajectory, contact pressures, and acoustic signatures. Analysis of the peak contact pressure and acoustic amplitude showed a modest, statistically significant correlation ( $r = 0.42$ ,  $p = 0.02$ ). A method to measure the gait stance time from features in the acoustic signature was tested. **Conclusions:** The results show that acoustic signals can be used to characterize gait changes, but additional work is needed to link acoustic signal features to gait events like toe lift.

**Keywords:** gait analysis; fatigue; footstep sound; plantar center-of-force; plantar pressure



Academic Editor: Tibor Hortobágyi

Received: 2 November 2024

Revised: 9 January 2025

Accepted: 11 January 2025

Published: 23 January 2025

**Citation:** Buxton, J.; Shields, K.J.; Greyshock, J.T.; Ramsey, J.; Adams, C.; Richards, G.A. Investigation of Acoustic Signals for Gait Analysis. *Biomechanics* **2025**, *5*, 7.

<https://doi.org/10.3390/biomechanics5010007>

**Copyright:** © 2025 by the authors. Licensee MDPI, Basel, Switzerland. This article is an open access article distributed under the terms and conditions of the Creative Commons Attribution (CC BY) license (<https://creativecommons.org/licenses/by/4.0/>).

## 1. Introduction

Audible footstep sounds can reveal features of human gait. For example, it is easy to recognize extreme bilateral asymmetry from the sound of an injured person limping. Coaches and trainers often encourage athletes to “run quiet” to reduce impact or improve running form. Various studies have shown that individuals can be identified from the unique sounds they make as they walk [1–3]. Several authors have investigated the use of footstep sounds as a diagnostic tool for human gait [4–8]. Recently, footstep sounds have been studied for home healthcare purposes to monitor gait changes that are indicative of fall risk in elderly populations [9]. An improved understanding of the relationship between gait mechanics and footstep sound could enable a low-cost diagnostic tool for identifying gait anomalies.

The goal of this study was to determine if fatigue changes in plantar contact pressure were evident in audible footstep sounds. A within-subject study was used to compare the contact pressure and sound signals of participants before and after an exhaustive fatigue protocol. Results show a modest correlation between increased contact pressure and the maximum acoustic amplitude ( $r = 0.42$ ,  $p = 0.02$ ). We also compare stance times measured using conventional methods versus a proposed acoustic method.

### 1.1. Review of Prior Literature

In addition to reviewing acoustic methods of gait analysis, we include a discussion of vibration and accelerometer methods because the signal processing schemes are similar. We also discuss “person identification”, i.e., the process of identifying an individual from their unique gait pattern. The person identification application does not usually seek biomechanical parameters that are useful for clinical gait assessments, but could be modified to do so, as discussed here.

#### 1.1.1. Footstep Sounds for Person Identification

Hori and Fukuda [1] showed how acoustic recordings could be used to identify an individual from as little as one foot strike. Four participants walked on a wooden floor while sound was recorded for 60 s. After separating the signals into discrete steps sounds, the mel frequency spectrogram of each strike was used to train a convolutional neural network (CNN) and support vector machine (SVM) to classify the sound signals. Using the trained models on additional test data, the CNN method had a 98% accuracy for person identification among the four individuals.

Algermissen et al. [2] studied the footstep sounds of five individuals walking in a semi-anechoic room. After separating the signals into discrete steps, the mel frequency cepstral coefficients were used as features to train a CNN. The trained network achieved a 98% accuracy for gait recognition. The authors also tested cases where two individuals wore different shoes. The trained classifier was not successful at identifying these subjects, demonstrating that acoustic gait recognition is affected by the type of footwear.

Cai et al. [3] developed and tested a series of data processing tools that could enable individual footstep identification in the presence of ambient background noise, such as speaking. In a test with 20 participants, accurate identification approached 90% when signal processing was used to remove the background noise from the processed signal. Unique to this work, the structure-borne sound (i.e., the vibration in the floor) was used in addition to the direct acoustic signal to estimate the distance to the foot impact.

#### 1.1.2. Footstep Sounds for Gait Analysis or Gait Training

Umair Bin Altif and co-workers [4] proposed that footstep sound could provide inexpensive data useful for clinical gait assessments. They recorded footstep sounds from ten subjects walking on an approximately elliptical path. Due to the sharp impulse peaks associated with footstep sounds, the authors bypassed typical short-time Fourier transforms to analyze the signals and instead focused on the envelope of the acoustic signals. Combined with additional transformations described in the paper, the recorded signals produced clear representations of acoustic bursts associated with aspects of foot contact, midstance support, and toe lift. The authors coined the phrase “acoustic gaits” and suggested that traditional qualitative gait analysis could be supplemented with quantitative data from the acoustic recording. The paper noted that future studies are needed to provide a comparison between acoustic gaits and quantitative biomechanical measures like ground reaction forces, vertical impact rates, etc.

To reduce impact during running, Tate and Milner [5] used footstep sound intensity as biofeedback in gait retraining. The study aimed to reduce the vertical impact loading rate (VILR), vertical average loading rate (VALR), and vertical impact peak (VIP). Fourteen runners participated in the study. Baseline impact loads were recorded using a force plate mounted on a runway; five successful running trials (where subjects made contact with one foot on the force plate) were recorded as subjects ran at a self-selected speed in their own running shoes. Subjects then completed a fifteen-minute treadmill session, where a tablet computer measured the sound intensity of footsteps. The tablet computer provided

immediate feedback on the sound intensity as runners were coached to “run quietly”. After the treadmill session, impact load measures were repeated in the same manner as the baseline, with runners instructed to continue quiet running. The results showed statistically significant ( $p \leq 0.001$ ) reductions of more than 20% in all three loading parameters for more than 80% of the participants. The authors suggested that further work is needed to assess the efficacy of acoustic gait retraining for return-to-play protocols after injury.

In a study of barefoot runners, Phan et al. [6] compared the peak sound amplitude to the measured peak vertical ground reaction force (vGRF) and vertical loading rate. Twenty-six male subjects ran at a speed of 5.0 m/s across a force plate with a motion capture system. The sound was recorded using a shotgun microphone positioned approximately 0.3 m from the side of the force plate. Runners completed a baseline trial (normal running form) to produce up to ten data points where the right foot struck the force plate. Next, the runners were instructed to run as quietly as possible and complete ten more running trials. The results showed that many of the runners adopted different foot strike patterns in quiet running, often transitioning to non-rear foot strikes. For individual runners, the quiet cases correlated with a reduction in the vGRF, loading rate, and sound amplitude. However, as a group, there was no strong correlation between the peak sound amplitude and the measured vGRF. This result is different from studies on sound amplitude from vertical drop landings, where a general correlation between impact sound and vGRF is typically reported [7].

Hung Au and co-workers [8] investigated sound intensity as runners were instructed to switch between rearfoot, midfoot, and forefoot strike patterns. A total of 15 male and 15 female runners were outfitted with identical shoes and ran across a force plate and motion capture system for ten successful trials in each foot strike pattern. Before data collection, the subjects were coached and practiced running in each foot strike pattern. A microphone near the force plate was used to record the sound. The results showed statistically different sound levels and frequency content for the three foot strike patterns, indicating that sound properties are related to how the foot contacts the ground. However, no correlation was found between the sound properties and the average or instantaneous loading rates.

Summoogum et al. [9] suggested that acoustic signals could be used to provide in-home gait analysis to monitor elderly adults at risk of fall injuries. To demonstrate the concept, temporal gait parameters (cadence, step time, and stride time) were recorded from 10 participants over 65 years of age (including some with known fall-risk potential). Forty steps were recorded from each participant. Inertial measurement units (IMUs) and video analysis were used to provide reference gait data and were then compared to acoustic measurements. Acoustic data were processed to find heel-strikes using an energy measure described in the paper. Following this procedure, the relative standard error between the reference and acoustic gait parameters was less than 1.2%, affirming the potential of acoustic gait measurements.

### 1.1.3. Vibration and Accelerometer Measures for Person Identification and Gait Analysis

Since the 1990s, the floor vibration caused by human footfalls has been used to detect people walking nearby [10]. More recently, several authors have investigated the use of floor vibration for person identification and as a gait analysis tool.

Hahm and Anthony [11] suggested that footfall floor vibrations may be useful for monitoring gait changes in older adults, providing early detection of neurocognitive disorders like Parkinson’s disease. Continuous monitoring at home provides walking data in a familiar setting, unaffected by clinical observation or a new environment. However, floor vibration signals are potentially confounded by multiple occupants walking at the

same time. To address this issue, the authors developed a signal processing method that can distinguish vibrations originating from two different walkers (with 94% accuracy) and then calculate individual step time, location, and estimated ground reaction force. These vibration-calculated parameters were compared to those from traditional motion capture or using measured tibial acceleration as a proxy for ground reaction force. Footfall vibration data were used to estimate step-time asymmetry and ground reaction force. The results showed root-mean-square error values of 3.4% and 9.1% for these respective parameters.

In a study of children with muscular dystrophies (MD), Dong et al. [12] compared traditional gait assessments to features extracted from floor vibrations generated as the participants walked. Data were collected for 36 participants (21 healthy and 15 with MD). A signal processing method and neural network were developed to analyze the vibrations, achieving a 94.8% accuracy in classifying the MD gait “stage” (i.e., the extent of MD disability). The authors suggested that the simplicity of using common geophones to record floor vibrations could allow routine measurement of MD progression.

Related studies on wearable IMUs (inertial measurement units) have shown that individuals have unique gait patterns that can be identified from the IMU signals. In a study of 81 participants, Wiles et al. [13] demonstrated unique gait patterns that identified individuals with an accuracy as high as 98.63% using a random forest classifier. Gait patterns were recorded with 16 inertial measurement units (IMUs) on the participants as they walked for 4-min on a 200 m indoor track. The authors suggested that IMU gait patterns may be analyzed for changes that accompany disease or injury, although they did not directly study this issue.

A unique approach to person identification was demonstrated by Koffman et al. [14]. Thirty-two participants wore accelerometers on their left wrist and walked outdoors for nine to fourteen minutes of data collection. Unlike other studies, the individual gait cycles were not “cut out” for analysis. Instead, 1.0 s segments were cut from the data, and then a series of time shifts was applied to each segment. The original versus time-shifted data were plotted, creating plots unique to each individual. Using methods described in the paper, the individual walkers were identified with 100% accuracy. The tests do not consider any specific biomechanical variables (like step time, ground reaction force, etc.) but the method could be further tested against these gait features.

### *1.2. Summary of Prior Studies*

Prior literature shows that low-cost sensors like wearable IMUs, accelerometers, microphones, and floor geophones can be used for person identification and some aspects of gait analysis. These sensor methods do not replace traditional gait analysis but could provide data for health monitoring or simplified test procedures. Sound signals can measure some gait aspects, but additional studies are needed to clarify the relationship between footstep sound and gait parameters.

## **2. Materials and Methods**

### *2.1. Experimental Setup*

The experimental setup was reported in a previous paper from our group [15], demonstrating that fatigue produces subject-specific changes in plantar pressure. This paper presents both acoustic signals and plantar pressures at jogging speed (2.7 m/s or 6 MPH). Acoustic signals were recorded with a conventional microphone (Shure SM57, [www.shure.com](http://www.shure.com)) located on the centerline of the treadmill (Trackmaster TMX425C, Newton, KS, USA). Referring to Figure 1, the microphone position D was referenced to a feature on the treadmill (the peak of the motor cover), with H measured from the ground. The axis of the microphone was angled approximately to meet the mid-point of the treadmill

running surface. The microphone signal was sent to a Focusrite Scarlett Solo Audio Interface ([www.focusrite.com](http://www.focusrite.com)) and then recorded on a laptop computer using the open-source software Audacity ([www.audacityteam.org](http://www.audacityteam.org)). Signals were captured at a standard audio recording frequency of 44.1 kHz. Information about the room acoustics is included in Appendix A.

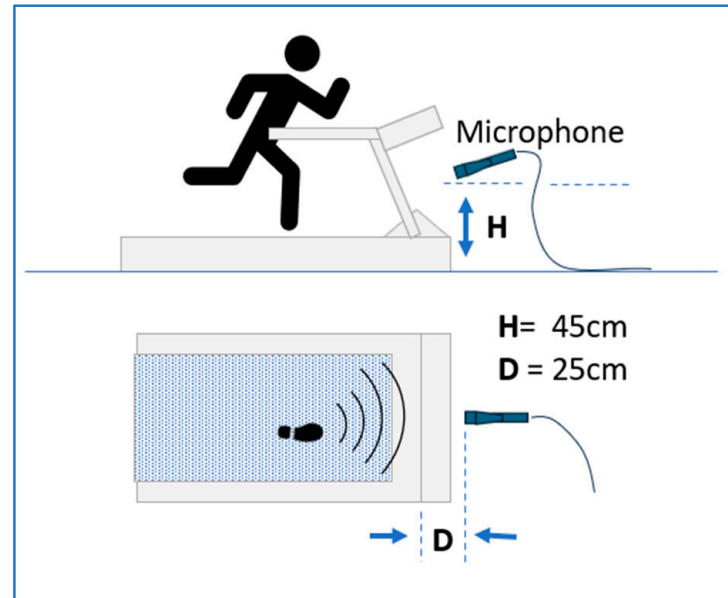


**Figure 1.** Experimental setup showing the position of the microphone relative to the treadmill. Variables H and D show the height and distance from the treadmill structure. Additional information regarding room acoustics and preliminary experimentation are included in Appendix A.

In-sole pressure sensors (3000 Sport-E 125, Tekscan, Boston, MA, USA) were used to measure plantar pressure and record the center of force (COF) trajectory and center of force-velocity (COF-V) for each footfall (Figure 2). The plantar pressure distribution was recorded at 400 Hz, producing approximately 120 frames per stance at jogging speed. Data were recorded using the F-Scan VersaTek Datalogger system and Tekscan Research Software (version V.7.55). The plantar sensor had a maximum pressure capability of 862 kPa and a resolution of 4.8 kPa. Individual sense elements (termed “sensiles”) were distributed uniformly across the plantar surface with 3.9 sensiles/cm<sup>2</sup>. Accuracy and repeatability have been assessed and reported previously [15–17]. Sensor durability was an issue at times, with some sensile elements failing (recording zero or anomalous pressure) during tests. To ensure representative measurements, each test case was manually inspected to confirm that less than 5% of the contact area was affected by sensile failure. Of the 30 test cases (15 participants, pre- and post-fatigue), two test cases exceeded this 5% limit (7% and 14%) but were retained in the dataset because these anomalies did not affect the recorded acoustic data.

For data analysis, we use the same nomenclature as in the F-Scan system. In this context, “contact pressure” refers to the total force under foot at any instance in time, divided by the area of foot contact. Thus, even with the same force, the contact pressure is greater if the foot contact area is less.  $CP_{max}$  is the largest value of contact pressure recorded from foot strike to toe lift. Force is the sum of individual forces measured by all sensiles. The force is related to—but not exactly the same as—the vertical ground reaction force due to the curvature underfoot on a flexible sensor [18].

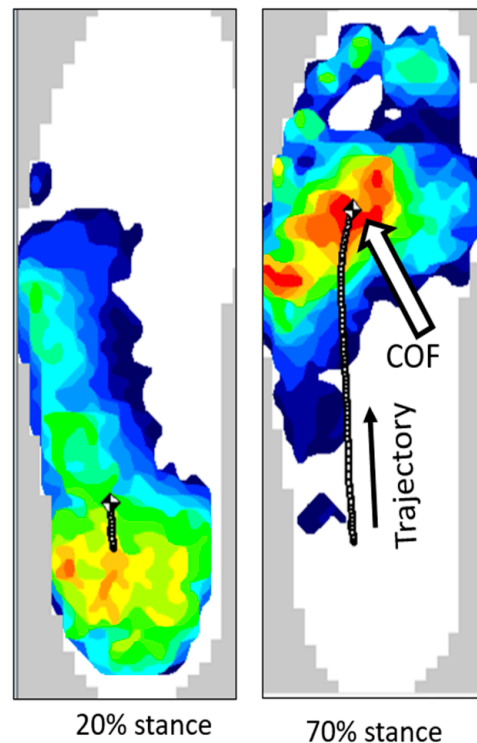


**Figure 2.** Example of left foot plantar pressure distribution. **Left:** 20% stance—shortly after heel contact. **Right:** 70% stance—approaching toe off. The center of force (COF) and trajectory are shown and reveal the foot rolling forward. The plantar pressures are proportional to the color scale with blue = low pressure and red = high.

## 2.2. Participants and Test Protocol

Participants were recruited using an inclusion criterion for runners averaging 10 to 30 miles per week and between the ages of 18 and 35 years. The resulting pool of participants included 16 individuals (7 male, 9 female) with a median age of 19 years and median body weight of 65.1 kg. Further demographic details are listed in [15]. Due to a microphone problem, data from one participant are not included in this paper, meaning there are 15 participants analyzed here. All participants were made aware of the risks and benefits of participation prior to providing their written informed consent. Participants used their own running shoes, including any foot orthosis.

The test protocol involved a sequence of treadmill walking, jogging, running, and sprinting (1.3, 2.7, 3.3, 4.5 m/s), with sixty seconds at each speed. This was followed by a fatigue protocol, and then the speed sequence was repeated. Only jogging cases are reported in this paper.

The fatigue protocol followed methods similar to Hamzavi and Esmaili [19]. Participants were monitored for heart rate (chest-strap, Polar Electro, Kempele, Finland), blood lactate (capillary finger-tip samples, Lactate Plus, Nova Biomedical, Waltham, MA, USA), and rate of perceived exertion (RPE, 6–20 Borg scale [20]). After baseline blood lactate measurements, participants began a 3.0 m/s run with zero grade. The speed increased by 0.2 m/s every two minutes. Speed increases continued until the participants reached RPE = 13. Participants maintained this speed for two minutes after reaching an RPE of 17 or 80% of their age-predicted maximum heart rate, at which point, the fatigue protocol ended. Blood lactate (BL) measurements confirmed substantial fatigue with an average increase of 6.1 times over baseline (std. dev. 2.6).

All procedures were approved by Grove City College IRB (no. 111-2021) prior to implementation and all testing occurred in the Exercise Science Laboratory of Grove City College.

### 2.3. Acoustic Signal Processing

Acoustic signals for each footfall were coordinated with the left versus right foot and with COF (center of force) and COF velocity (COF-V), as shown in Figure 3. The stances defined by the COF-V signal allowed for the partitioning of the acoustic signal for averaging left and right foot strikes. The acoustic signal envelope was used to characterize the sound amplitude profile during foot strike. An RMS envelope was calculated in MATLAB [21] with a sliding window length of 400 data points. The application of a 400 data point sliding window to a 44.1 kHz acoustic signal implied a window interval of 9.1 milliseconds. This interval was less than 4% of the typical stance time (250–300 milliseconds). Tests of different windows confirmed that 400 data points reduced noise from high-frequency processes while providing good resolution of amplitude features from foot contact. Among the envelope methods (Hilbert, analytic, or peak), RMS was selected because it represents signal energy content. To create an ensemble average, software was written in MATLAB to identify the time at the center of a left stance ( $t_c$ ) and the duration of that stance ( $T_d$ ) in seconds. An ensemble element was defined for the time interval ( $t_c - 1.5T_d$ ) to ( $t_c + 1.5T_d$ ) as shown in Figure 3. A left-foot ensemble average was thereby calculated simply by recording elements from all left footsteps and averaging the elements. Equivalent elements could be defined with the right-centered elements or centered anywhere on the pattern. Aside from using the RMS envelope as described, the acoustic signal was not otherwise filtered. The typical ensemble length was 0.8 s. With the sampling rate of acoustic recording (44,100 Hz), each ensemble included more than 35,000 points of time series data.

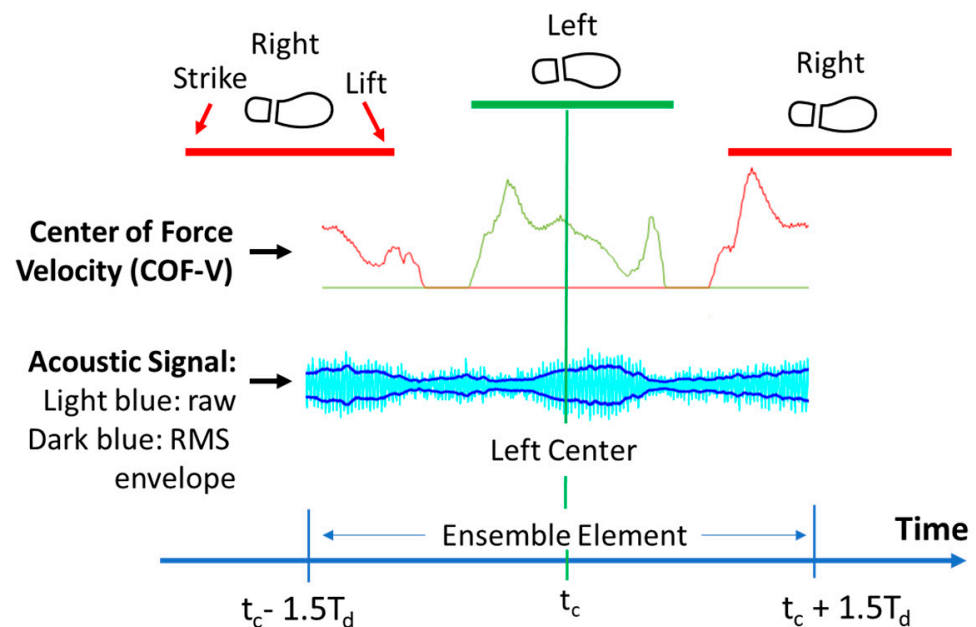


**Figure 3.** Method to create the ensemble average of acoustic signals based on the left foot contact. The COF-V signal was used to detect the left or right stances. A COF-V equal to zero occurs when neither foot is on the treadmill. A non-zero COF-V indicates the stance phase, shown as a horizontal green/red line where the COF-V  $\neq 0$  for right/left stances. Compared to plantar pressure, COF-V was the preferred method of detecting the stance phase due to excessive signal noise when using plantar pressure alone. The raw acoustic signal (light blue) and the RMS envelope (dark blue) are shown.

#### 2.4. Addressing Latency Between COF-V and the Acoustic Signal

The COF-V and acoustic signals were recorded by two different pieces of software, leading to signal latency [22]. The recorded acoustic signal may slightly lag or lead to the actual COF-V due to software initiation differences. Various attempts to estimate the latency (e.g., from single impulse measurements such as a single foot stomp) revealed that latency was typically less than 0.07 s. A latency correction was applied to the data to account for the fact that the sound envelope decreased when both feet were in the air and increased with a foot contacting the treadmill. The acoustic signal increase with foot contact was easily identifiable. Also of note, despite the acquisition latency, the durations of the stance and swing phases were correctly recorded as measured from the COF-V plot. The latency correction only modified the phase between the acoustic signal and COF-V.

#### 2.5. Statistical Analysis

The primary dependent variables are the maximum values of the contact pressure,  $CP_{\max}$ , and the maximum acoustic amplitude,  $AA_{\max}$ . We will also report the maximum force,  $F_{\max}$ . Maximum values were derived from the peaks in the ensemble average of more than sixty footstep ensemble elements.

Statistical analyses were performed using SPSS (IBM SPSS Statistics, V 28.0.1.0). For all reported data, normality was affirmed from a Shapiro–Wilk test at a 0.05 level of significance and further validated by inspecting a Q-Q plot. For all statistical tests, ( $p$ ) < 0.05 was considered statistically significant, a priori. Paired, one-sided  $t$ -tests were used to compare changes between pre- and post-fatigue  $AA_{\max}$  and  $CP_{\max}$  with the effect size reported as corrected Hedges'  $g$ . The Pearson correlation between  $CP_{\max}$ ,  $AA_{\max}$ , and  $F_{\max}$  is reported with the standard  $r$  and  $p$  values calculated in SPSS.

### 3. Results

#### 3.1. Center of Force Observations for Five Participants

Figures 4 and 5 show the COF observations and acoustic envelopes for five randomly selected participants. These graphs are included to graphically show the COF appearances and acoustic data. Similar plots are available for ten additional participants in the Supplementary Material. In the data that follow, COF data points are only plotted when the force is greater than 30% of the maximum, thus minimizing spurious sensor noise that occurs at the start and end of foot contact.

The COF trajectories for five participants A–E are shown in Figure 4 for pre- and post-fatigue. There are marked differences in shape and variability between pre- and post-fatigue and between participants. Considering Participant A, pre-fatigue, we see a maximum variation of ~1 cm in the medial–lateral direction. The COF progresses from 1 to 2, starting with a slight lateral hook, and then almost vertically from 2 to 3. The foot then rolls medially, and toe lift occurs at 4.

Considering post-fatigue for Participant A, the trajectory changes in several ways, including the absence of the lateral turn at foot strike (no hook). In addition, the main trajectory now slants slightly left of vertical. The trajectory moves medially until toe lift, like pre-fatigue, but with some additional variability. The maximum force is greater for post-fatigue and occurs earlier in the stance phase when compared to pre-fatigue.

Inspecting Participants B to E reveals additional COF trajectory differences for pre- vs. post-fatigue and between participants. Of particular interest is Participant E, where the runner is a forefoot striker pre-fatigue, but then settles into a rear-foot strike pattern post-fatigue.

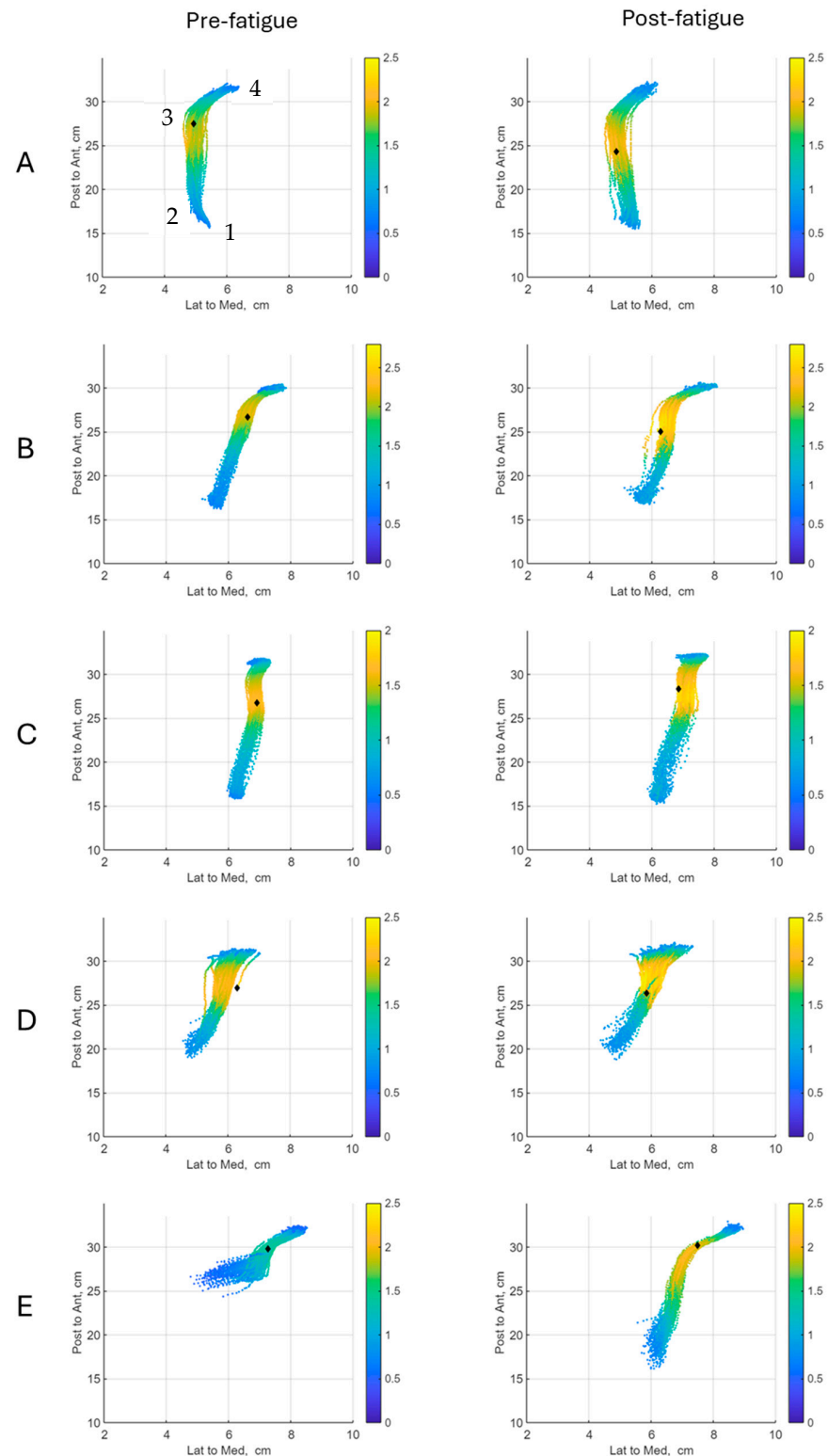


**Figure 4.** (A–E): Left foot COF trajectory. Column 1: pre-fatigue; Column 2: post-fatigue. Force is indicated by the color scale as a ratio to body weight (BW). Each plot is approximately 70–80 stances (individual steps). Path trajectory sequence labeled 1 to 4 shown in Case A; see the text for discussion. The color scale is the same for pre- and post-fatigue comparisons in a participant, but the color maximum (bright yellow) is set to match the peak force observed in an individual. A black dot on each plot indicates the position where the largest force is recorded. The Supplementary Information includes ten additional participants.

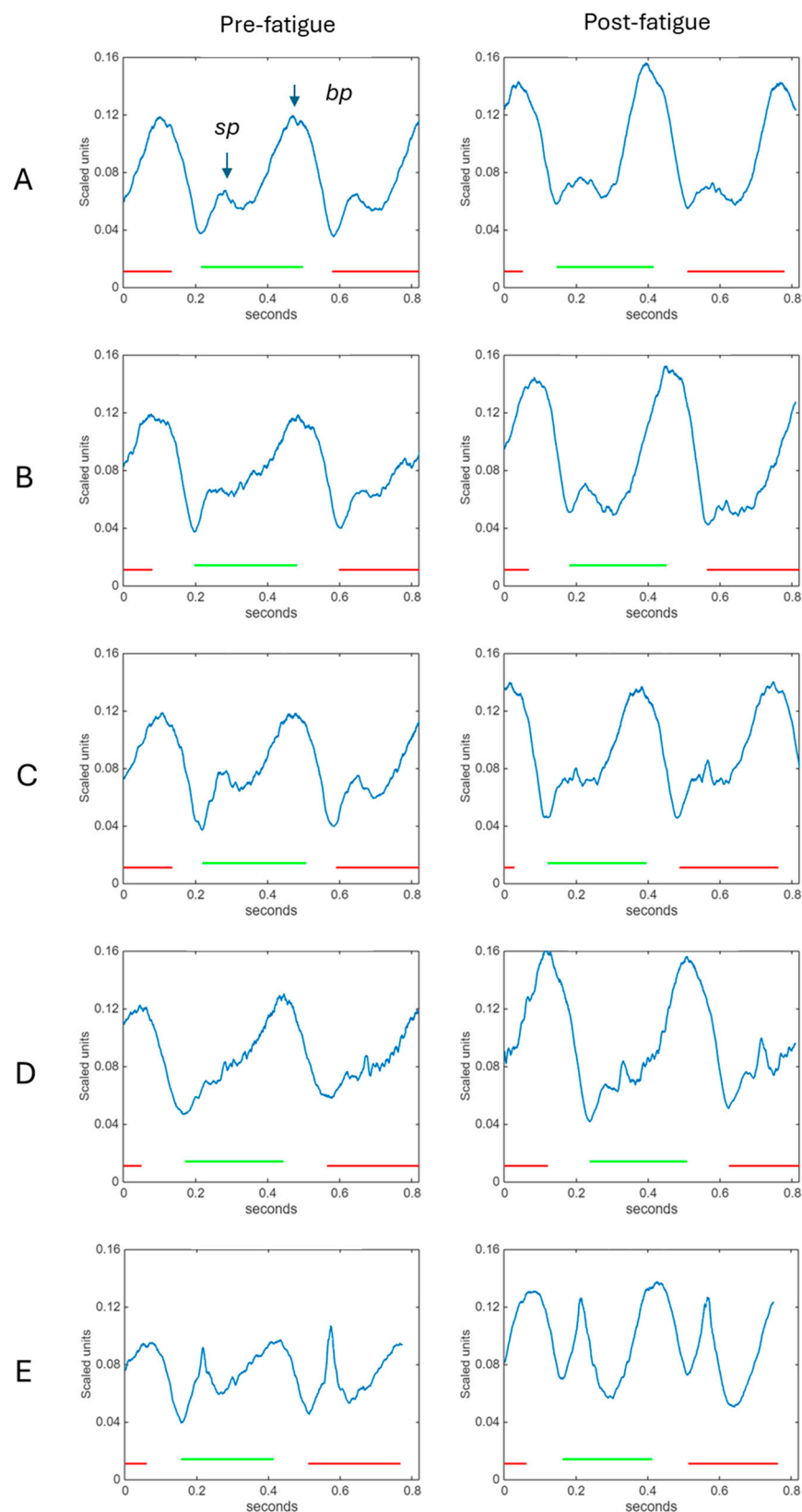


**Figure 5.** Ensemble-averaged acoustic envelopes, subjects (A–E). For both pre- and post-fatigue, the green/red (left/right) stance markers are corrected for latency, assuming the sound level rises when the foot strikes. The figures are characterized by small and big peaks (sp, bp), a consistent bp right-side decline, and an increase in amplitude with fatigue. See the Supplementary Information for an additional ten participants.

Similar figures for an additional ten participants are included in the Supplementary Information. A detailed analysis of these figures is warranted to understand how fatigue modifies gait, but the focus here is to determine if the modified gait is evident in the corresponding acoustic signals, discussed next.

### 3.2. Acoustic Signal Observations of Five Participants

Figure 5 presents the average acoustic envelope corresponding to each case shown in Figure 4. Starting with Participant A, pre-fatigue, the signature shows two distinct features associated with each stance: a small peak (sp) and a big peak (bp). We define the magnitude at bp as  $AA_{max}$ , the maximum acoustic amplitude. Post-fatigue,  $AA_{max}$  is greater when compared to pre-fatigue, and the slope rising to bp is steeper. Qualitatively, the overall shape of sp pre-fatigue is skewed right but appears symmetrical post-fatigue. Similar shape and magnitude changes for post-fatigue are evident for Participants B–D. Fatigue increases the magnitude and leading slope of bp and is accompanied by a more symmetric sp. Case D appears to be missing the sp before fatigue, but the sp emerges after fatigue. Participant E (the forefoot striker) also has two prominent features, but the sizes of the sp and bp are very similar, and the magnitudes of sp and bp both increase with fatigue. As with the other cases, the slope leading to the bp is increased by fatigue. Among all cases, the behavior after bp appears similar for both pre- and post-fatigue cases. We suggest that the smooth decline to the minimum represents the decay of acoustic energy when both feet are off the treadmill.

### 3.3. Maximum Contact Pressure, Acoustic Amplitude, and Force

We will now analyze the maximum values of acoustic amplitude,  $AA_{max}$ , contact pressure,  $CP_{max}$ , and force,  $F_{max}$ . Referring to Figure 6A,B, plots of post-fatigue versus pre-fatigue show increases in both  $CP_{max}$  and  $AA_{max}$  for most participants. Graphical increases are statistically confirmed with paired, one-sided  $t$ -tests, yielding  $p$ -values of  $p = 0.01$  for  $CP_{max}$  and  $p < 0.001$  for  $AA_{max}$ . The size effects, expressed as Hedges'  $g$ , are  $g = 1.83$  for  $AA_{max}$  and  $g = 0.49$  for  $CP_{max}$ . A moderate correlation exists between the two parameters ( $r = 0.42$ ,  $p = 0.02$ ); see Figure 7.

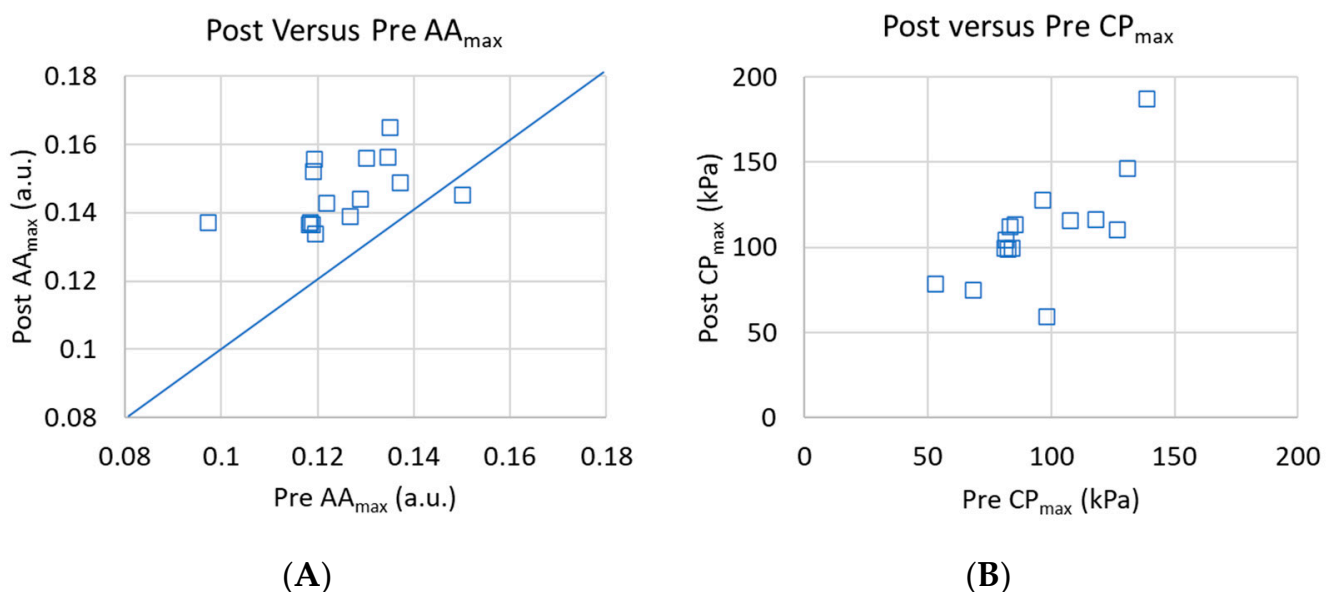


**Figure 6.** Post- versus pre-fatigue comparisons: (A) maximum acoustic amplitude,  $AA_{max}$ , (B) maximum contact pressure,  $CP_{max}$ . The blue line shows equal pre- and post-fatigue values.

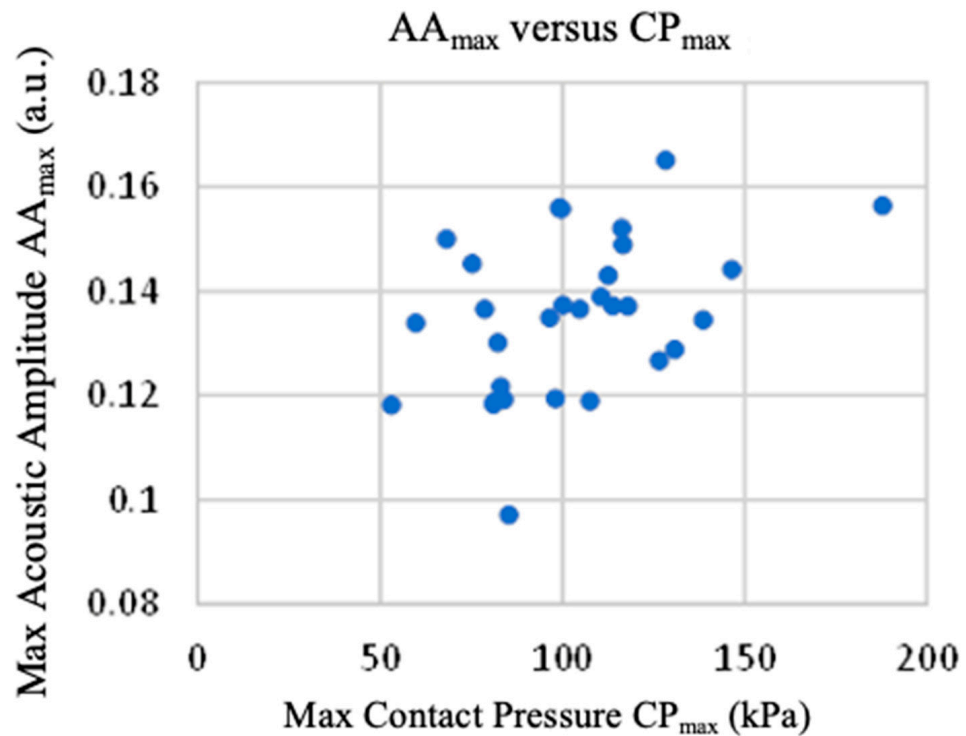


**Figure 7.** Comparison of maximum acoustic amplitude and contact pressure. Fifteen participants, (pre- and post-fatigue cases) are included. Pearson correlation for all data points,  $r = 0.42$ ,  $p = 0.02$ .

Other factors that might be expected to correlate with  $AA_{\max}$  were also investigated (Table 1). The peak force,  $F_{\max}$ , measured during each stance, correlates with  $CP_{\max}$  ( $p = 0.01$ ) but not with  $AA_{\max}$  ( $p = 0.22$ ). Additionally, as expected, there is a significant correlation between the participant's weight and  $F_{\max}$  ( $p < 0.0001$ ).

**Table 1.** Pearson correlation coefficient matrix ( $r$ ,  $p$ -value). \*  $p < 0.05$ , \*\*  $p < 0.01$ .

	$AA_{\max}$	$CP_{\max}$	$F_{\max}$	Weight
$AA_{\max}$	1			
$CP_{\max}$	0.42, 0.02 *	1		
$F_{\max}$	0.23, 0.22	0.46, 0.01 **	1	
Weight	-0.14, 0.48	0.01, 0.97	0.73, <0.001 **	1

$AA_{\max}$  = max. acoustic amplitude.  $CP_{\max}$  = max. contact pressure.  $F_{\max}$  = max. force during stance. Weight = participant weight.

### 3.4. Temporal Gait Metrics from Acoustic Signals

The plantar pressure sensors can be used to directly measure cadence and stance times (Figure 3). Are we able to derive similar metrics from the acoustic signal? The average cadence can be easily determined via acoustics from the time difference between the big peaks (bp) or directly by counting the familiar step “sounds”. However, it is more difficult to use acoustics to determine the stance time (the time between foot contact and toe lift). Foot contact can be recognized in the acoustic signal with the assumption that contact produces an abrupt increase in sound amplitude. This feature identifies a clear start to the foot contact. However, the toe lift is more gradual and is confounded by decaying acoustic reflections (see Appendix A) and sound generated by the treadmill belt during the toe lift.

Despite these uncertainties, we investigated an acoustic measurement of the stance time compared to the plantar sensor. Referring to Figure 8, distance F represents the actual stance time as recorded by the pressure sensor, while the maximum big peak (bp max) for

the acoustic signal is marked with an inverted triangle. We designate the time between foot contact and bp max as A. Note that bp max may not be precisely aligned with the end of the foot contact. The last few moments of foot contact include sound generation from the toe lift after the bp max and potentially some processes as the treadmill belt reacts to pressure release. However, if the toe lift consistently lags behind the acoustic peak, the A/F ratio could provide a useful way to calculate the foot contact time, F, from the acoustic measure, A. To test this possibility, the boxplot shows the A/F ratios for all participants, pre- and post-fatigue. While there are some notable outliers, the mean value is 0.92, with 95% confidence intervals of [0.89, 0.95]. Thus, the stance time, F, can be estimated as  $F_{\text{est}} \approx A/0.92$ .

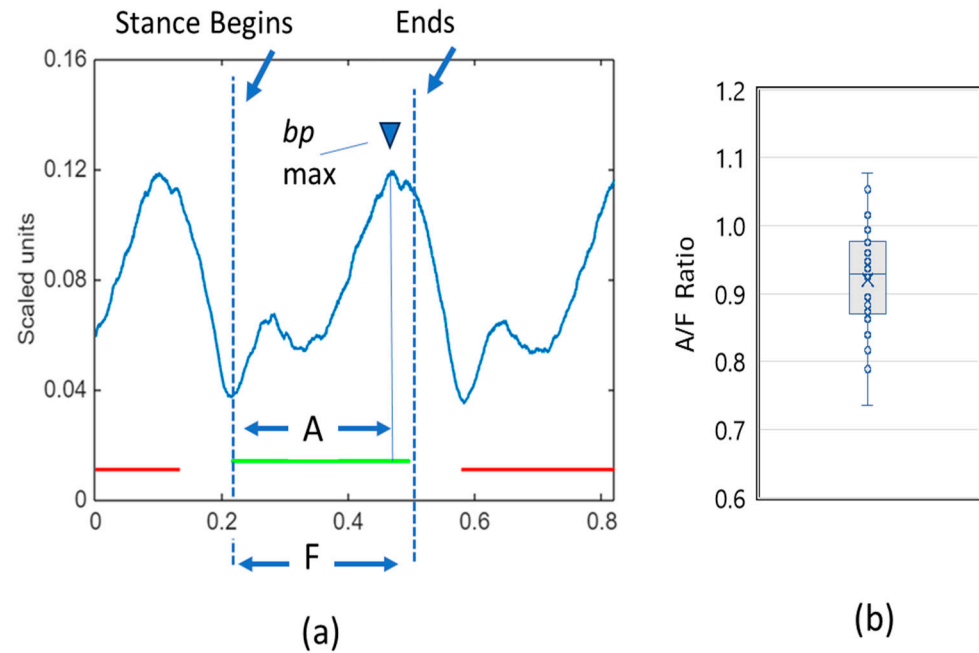


**Figure 8.** Analysis of pressure sensors with acoustic signals. Green/red lines show pressure sensor measurement of stance for left/right foot. (a) The pressure sensors measure the full stance (F) and the microphone detects the bp max of the acoustic signal. The new measure (A) is the time between foot contact and bp max (Participant A, pre-fatigue). (b) Box plot of the A/F ratio for each participant (includes both pre- and post-fatigue).

#### 4. Discussion

The acoustic emission generated by an impact event is known to increase with the impact force and rate [23]. Thus, high-impact foot strikes should produce higher acoustic amplitudes. In our study of 15 participants, we found a moderate correlation between the maximum contact pressure ( $CP_{\text{max}}$ ) and acoustic signal ( $AA_{\text{max}}$ ). Other studies have reported different relationships between sound amplitude and gait properties. Phan et al. [6] instructed runners to “run quiet”, which resulted in significant reductions in both sound amplitude and vertical ground reaction force in *individuals*. However, across all runners, there was a poor correlation between sound and force. Our results also show a poor correlation between sound amplitude and *force*, but a modest correlation between sound amplitude and *contact pressure*. Thus, future studies on footstep sound generation may benefit from analyzing plantar pressure, not just force. Hung Au et al. [8] showed that sound levels were different when runners were coached to use different foot strike patterns (rear, mid, and forefoot). Although our study did not focus on foot strike patterns, the results show a very different shape sound envelope with one forefoot striker (Participant E, see Figures 4 and 5), but fewer differences in another (Participant J, see Supplementary Information). We also

note significant experimental differences when compared to prior studies. We used fatigue to produce gait changes, while both [6,8] instructed participants to change their own gait patterns. Another difference is that this study analyzed acoustic data from treadmill testing. While the treadmill introduced mechanical noise, it also provided many steps for analysis, likely improving data consistency.

The measured stance times versus acoustic estimates lacked the desired precision. Our group is currently using high-speed video and synchronized audio to identify the features of acoustic amplitude and frequency that characterize toe lift. An accurate acoustic indicator of heel strike and toe lift would enable acoustic measures of stance time, swing time, and step variability.

For the data presented here, plantar pressure sensors were used to identify the start and stop times for acoustic ensemble elements. We also successfully tested an acoustic peak-finding algorithm to identify ensemble elements from the acoustic signal alone. In essence, the “thump” of each foot strike was used to define the ensemble elements. The resulting ensemble averages were similar to those using the plantar pressure, indicating the potential of the sound recording alone as a gait diagnostic.

A future goal for our research includes training a model to predict gait features from the corresponding acoustic signal. The literature cited earlier shows that machine learning models can be trained to characterize some aspects of gait. Acoustic person identification has focused on the spectral features of the signals. The mel spectrum [1] or the coefficients of the mel frequency cepstrum [2,3] have been used as features to train convolutional neural networks to recognize individual gait patterns.

In contrast to person identification, acoustic gait analysis has few precedents in the literature for selecting features and model approaches. Summoogum et al. [9] used the mel spectrogram (and acoustic energy) to accurately identify the timing of heel strikes during walking but did not train any models. Using floor vibration signals (not acoustics), Hahm and Anthony [11] used a modified Gaussian mixture model to accurately classify left versus right foot impacts, providing a method to measure step times.

Given many potential model approaches, we are currently evaluating the best method to link gait features to the sound signal. Umair Bin Altif [4] encouraged the use of acoustic envelopes to characterize footstep sounds, noting that time–frequency uncertainty [24] places limitations on timing brief impact sounds in spectrograms. This uncertainty apparently did not limit the timing of heel strikes [9] and has not been an issue for the person identification algorithms mentioned above. Recent studies on industrial acoustic diagnostics use neural network image classification of mel spectrograms to identify machinery conditions [25]. At present, we are investigating both the envelope and spectral methods to identify consistent acoustic features needed to train a model.

### *Limitations*

As discussed, latency in signal capture was due to the use of separate collection devices (pressure and acoustic). The correction for this latency was based on the reasonable assumption that acoustic amplitude should rise with foot contact. Eliminating the signal latency would allow for direct comparison of raw acoustic and plantar pressure signals, providing a better opportunity to link features in both signals. Our group is currently developing a synchronizing method that records the various signals with a common time stamp.

Participants in this study used their own running shoes. Different shoes will produce different sound levels [2]. More consistent data would be expected by having all participants use the same type of shoe or run barefoot, as in [6,8]. However, this study focused on within-participant variation, with the same shoe, before and after fatigue. Comparisons

between participants need to consider potential differences due to the type of shoe. Aside from different shoes, the very specific acoustic envelope for some participants (e.g., forefoot runner) adds to data variability. Future studies may be segregated into foot strike types.

Another limitation is the treadmill itself. Because the sound generation includes foot interactions with the treadmill belt and deck, results may be different on other treadmills or running surfaces. Studies on these different surfaces are being conducted by our group to assess the limitations. We have shown that the interpretation of the ensemble-average acoustic signal is unaffected by background noise such as talking, walking, etc. The ensemble-averaging process reduces these uncorrelated sounds to a negligible average contribution among more than 60 correlated ensemble elements. This observation suggests that acoustic recordings could be taken in a clinical environment without the need for complete silence.

## 5. Conclusions

In conclusion, this paper demonstrates the potential of acoustic recording as a low-cost diagnostic tool for analyzing human gait. We show a moderate correlation between the contact pressure and the acoustic signal, as well as an acoustic method to estimate stance time. The complex process of sound generation during the foot strike presents a challenge in identifying features like toe lift within the sound envelope. Ongoing efforts will combine both envelope and spectral methods to identify features and use machine learning to connect acoustic features with gait characteristics.

**Supplementary Materials:** The following supporting information can be downloaded at <https://www.mdpi.com/article/10.3390/biomechanics5010007/s1>, Figure S1. COF Trajectory Participants F–J, Figure S2. COF Trajectory, Participants K–O, Figure S3. Acoustic Envelopes Participants F–J, Figure S4. Acoustic Envelopes Participants K–O, Table S1. Data used to generate Figures 6 and 7 and Table 1 in the main text.

**Author Contributions:** K.J.S.—formal analysis, writing—original document, writing—review and editing; G.A.R.—conceptualization, formal analysis, methodology, supervision, writing—original document, writing—review, and editing; J.B.—conceptualization, methodology, writing—review and editing; J.T.G.: signal processing methodology; C.A.—fatigue protocol methodology; J.R.—supervision. All authors have read and agreed to the published version of the manuscript.

**Funding:** Plantar pressure sensors used in this research were funded by Highmark Health.

**Institutional Review Board Statement:** This study was conducted in accordance with the Declaration of Helsinki and approved by the Institutional Review Board (or Ethics Committee) of Grove City College (protocol code 111-2021 22 Sept. 2021).

**Informed Consent Statement:** Informed consent was obtained from all participants involved in the study.

**Data Availability Statement:** Research data are available upon request.

**Acknowledgments:** Data reported in this study were collected with the help of a team of undergraduate students under the direction of authors Richards and Buxton. The dedication and commitment of these students is gratefully acknowledged.

**Conflicts of Interest:** Author Jesse T. Greyshock was employed by Bell Textron Inc. The remaining authors declare that the research was conducted in the absence of any commercial or financial relationships that could be construed as a potential conflict of interest.

## Appendix A

Appendix A considers the effect of room acoustics on the measured sound amplitude. Reflected acoustic energy will contribute to features in the acoustic signals, so more work is

needed to demonstrate the role of reflected acoustic energy on the sound signals. Modest efforts were made to dampen reflected waves in this study, especially because of the small room, but anechoic testing would be impractical for a clinical diagnostic.

The treadmill was located in a lab room with dimensions of  $5.2 \times 2.7 \times 3.4$  m (L, W, H). To minimize the effect of acoustic reflections, the floor was covered with standard foam gym flooring tile. The walls were covered with acoustic ceiling tiles, up to a height of 1.8 m. While it may be argued that genuine anechoic wall tiles would further reduce reflected sound, this was not pursued because the largest, closest reflecting surface is the treadmill, which cannot be covered. To understand the effect of reflected acoustics, we used repeated hand claps near the treadmill walking surface as impulse sources and recorded the response. Clap recordings [26] were made without the treadmill running, and the room was otherwise quiet. Figure A1a shows four clap impulses, and A1b shows a close-up. The x- and y-axes in the close-up use the same scale applied throughout the paper for presenting acoustic envelopes of footstep sounds. The y-axis is scaled to a  $5\times$  sound signal, recorded by Audacity using the SM57 microphone and Scarlett interface at full gain. The  $5\times$  gain, a convenience for plotting sound with other variables, is the same gain factor used elsewhere in this paper.

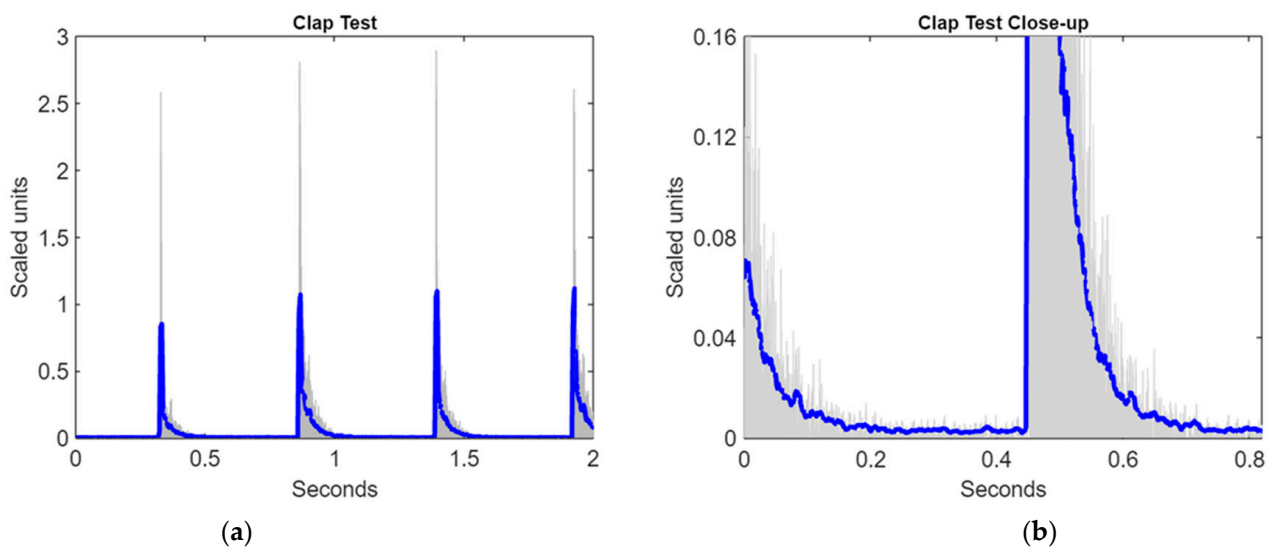


**Figure A1.** Acoustic recording of the clap test. (a) 2 seconds of data, four claps. (b) Close-up view of consecutive claps. The gray line denotes the raw signal. Dark blue denotes the root-mean-square envelope.

Focusing on Figure A1a, the light gray lines show the positive values of the recorded impulse sound signal. For simplicity, only the positive waveform is shown because the signal is symmetric about  $y = 0$ . The dark blue line shows the root-mean-square (RMS) envelope. Four impulse signals (“claps”) are shown in A1a; note that the sharp peaks are much larger than the RMS values, as expected. In the close-up, the discrete acoustic signals are tightly bunched under the envelope, with some discrete cycles evident around the blue line.

The right side of the RMS impulse envelope reflects the decaying sound amplitude following the impulse. The sound does not immediately “drop off” after the impulse, but decays as reflections are dissipated. For jogging or running, where both feet are momentarily off the treadmill, we might expect to see a consistent decay curve at the start of the swing phase, because the sound generated by the foot contact momentarily ceases.

## References

1. Hori, Y.; Ando, T.; Fukuda, A. Personal Identification Methods Using Footsteps of One Step. In Proceedings of the Conference on Artificial Intelligence in Information and Communication (ICAIC), Fukuoka, Japan, 19–21 February 2020. [CrossRef]
2. Algermissen, S.; Hörnlein, M. Person Identification by Footstep Sound Using Convolutional Neural Networks. *Appl. Mech.* **2021**, *2*, 257–273. [CrossRef]
3. Cai, C.; Jin, R.; Nie, J.; Kang, J.; Zhang, Y.; Luo, J. PURE: Passive Multi-Person Identification Via Footstep for Mobile Service Networks. *IEEE Trans. Veh. Technol.* **2023**, *72*, 12221–12233. [CrossRef]
4. Umair Bin Altaf, M.; Butko, T.; Juang, B.-H. Acoustic Gaits: Gait Analysis With Footstep Sounds. *IEEE Trans. Biomed. Eng.* **2015**, *62*, 2001–2011. [CrossRef] [PubMed]
5. Tate, J.J.; Milner, C.E. Sound-Intensity Feedback During Running Reduces Loading Rates and Impact Peak. *J. Orthop. Sports Phys. Ther.* **2017**, *47*, 565–569. [CrossRef]
6. Phan, X.; Grisbrook, T.L.; Wernli, K.; Stearne, S.M.; Davey, P.; Ng, L. Running Quietly Reduces Ground Reaction Force and Vertical Loading Rate and Alters Foot Strike Technique. *J. Sports Sci.* **2017**, *35*, 1636–1642. [CrossRef]
7. Wernli, K.; Ng, L.; Phan, X.; Davey, P.; Grisbrook, T. The Relationship Between Landing Sound, Vertical Ground Reaction Force, and Kinematics of the Lower Limb During Drop Landings in Healthy Men. *J. Orthop. Sports Phys. Ther.* **2016**, *46*, 194–199. [CrossRef]
8. Hung Au, I.P.; Ng, L.; Davey, P.; So, M.; Chan, B.; Li, P.; Wong, W.; Althorpe, T.; Stearne, S.M.; Cheung, R. Impact Sound Across Rearfoot, Midfoot, and Forefoot Strike During Overground Running. *J. Athl. Train.* **2021**, *56*, 1362–1366. [CrossRef] [PubMed]
9. Summoogum, K.; Das, D.; Efstratiou, C.; Palaniappan, R.; Jayakumar, P.; Wall, J. Passive Tracking of Gait Biomarkers in Older Adults: Feasibility of an Acoustic Based Approach for Non-Intrusive Gait Analysis. In Proceedings of the 2023 IEEE 19th International Conference on Body Sensor Networks (BSN), Boston, MA, USA, 9–11 October 2023; pp. 1–4. [CrossRef]
10. Museum Waalsdorp. Footfall Detector (1992–1995). Available online: <https://www.museumwaalsdorp.nl/en/museum-waalsdorp-2/other-2/other-footfall-detector/> (accessed on 18 October 2024).
11. Hahm, K.S.; Anthony, B.W. Machine Learning-based Gait Health Monitoring for Multi-Occupant Smart Homes. *Internet Things* **2024**, *26*, 101154. [CrossRef]
12. Dong, Y.; Iammarino, M.; Liu, J.; Codling, J.; Fagert, J.; Mirshekari, M.; Lowes, L.; Zhang, P.; Noh, H.Y. Ambient Floor Vibration Sensing Advances the Accessibility of Functional Gait Assessments for Children with Muscular Dystrophies. *Sci. Rep.* **2024**, *14*, 10774. [CrossRef] [PubMed]
13. Wiles, T.M.; Kim, S.K.; Stergiou, N.; Likens, A.D. Pattern Analysis Using Lower Body Human Walking Data to Identify the Gaitprint. *Comput. Struct. Biotechnol. J.* **2024**, *24*, 281–291. [CrossRef] [PubMed]
14. Koffman, L.; Zhang, Y.; Harezlak, J.; Crainiceanu, C.; Leroux, A. Fingerprinting Walking Using Wrist-Worn Accelerometers. *Gait Posture* **2023**, *103*, 92–98. [CrossRef] [PubMed]
15. Buxton, J.; Shields, K.J.; Nhean, H.; Ramsey, J.; Adams, C.; Richards, G.A. Fatigue Effects on Peak Plantar Pressure and Bilateral Symmetry During Gait at Various Speeds. *Biomechanics* **2023**, *3*, 310–321. [CrossRef]
16. Giacomozzi, C. Appropriateness Of Plantar Pressure Measurement Devices: A Comparative Technical Assessment. *Gait Posture* **2010**, *32*, 141–144. [CrossRef]
17. Patrick, K.; Donovan, L. Test–Retest Reliability of the Tekscan® F-Scan® 7 in-Shoe Plantar Pressure System During Treadmill Walking in Healthy Recreationally Active Individuals. *Sports Biomech.* **2018**, *17*, 83–89. [CrossRef]
18. DeBerardinis, J.; Trabia, M.B.; Dufek, J.S.; Le Gall, Y.; Da Silva Sacoto, N. Enhancing the Accuracy of Vertical Ground Reaction Force Measurement During Walking Using Pressure-Measuring Insoles. *J. Biomech. Eng.* **2020**, *143*, 011010. [CrossRef] [PubMed]
19. Hamzavi, B.; Esmaeili, H. Effects of Running-Induced Fatigue on Plantar Pressure Distribution in Runners with Different Strike Types. *Gait Posture* **2021**, *88*, 132–137. [CrossRef] [PubMed]
20. Borg, G. Psychophysical Bases of Perceived Exertion. *Med. Sci. Sports Exerc.* **1982**, *14*, 377–381. [CrossRef] [PubMed]
21. MATLAB, version 9.13.0 (R2022b); The MathWorks Inc.: Natick, MA, USA, 2022. Available online: <https://www.mathworks.com> (accessed on 2 November 2024).
22. Low Latency Audio—Windows Drivers. Available online: <https://learn.microsoft.com/en-us/windows-hardware/drivers/audio/low-latency-audio> (accessed on 27 May 2024).
23. Ross, A.; Ostiguy, G. Propagation of the Initial Transient Noise From an Impacted Plate. *J. Sound Vib.* **2007**, *301*, 28–42. [CrossRef]
24. Gröchenig, K. Time-Frequency Analysis and the Uncertainty Principle. In *Foundations of Time-Frequency Analysis. Applied and Numerical Harmonic Analysis*; Birkhäuser: Boston, MA, USA, 2001. [CrossRef]
25. Dalmia, S.; Rege, M. Anomalous Sound Pattern Detection for Machine Health Monitoring. In *Artificial Intelligence and Knowledge Processing. Communications in Computer and Information Science, Proceedings of the 3rd International Conference on Artificial Intelligence and Knowledge Processing, AIKP 2023 Rodriguez, Hyderabad, India, 6–8 October 2023*; K, H., Rodriguez, R.V., Rege, M., Piuri, V., Xu, G., Ong, K.L., Eds.; Springer: Berlin/Heidelberg, Germany, 2024; Volume 2127. [CrossRef]

- 
26. Seetharaman, P.; Tarzia, S. The Hand Clap as an Impulse Source for Measuring Room Acoustics. In Proceedings of the Audio Engineering Society 132nd Convention, Budapest, Hungary, 26–29 April 2012.

**Disclaimer/Publisher’s Note:** The statements, opinions and data contained in all publications are solely those of the individual author(s) and contributor(s) and not of MDPI and/or the editor(s). MDPI and/or the editor(s) disclaim responsibility for any injury to people or property resulting from any ideas, methods, instructions or products referred to in the content.